

Non-Newtonian hydrodynamic modes in two-dimensional electron fluids

Serhii Kryhin and Leonid Levitov

Department of Physics, Massachusetts Institute of Technology, Cambridge, MA 02139

(Dated: August 15, 2023)

Two-dimensional electron systems is an appealing platform to explore long-lived excitations arising due to collinear carrier scattering enabled by fermion exclusion and phase-space constraints. Recently it was shown that the lifetimes of these excitations surpass the fundamental bound set by Landau's Fermi-liquid theory by a factor as large as $(T_F/T)^\alpha$ with $\alpha \approx 2$. Long-lived degrees of freedom possess the capability to amplify the response to a weak perturbation, producing lasting collective memory effects. This leads to nonclassical hydrodynamics in 2D electron fluids driven by multiple viscous modes with non-Newtonian viscosity not anticipated by previous work. We describe these modes as Fermi surface modulations of odd parity evolving in space and time, and discuss their experimental implications.

Recent years have seen a surge of interest in Gurzhi's electron hydrodynamics [1] as a framework to describe transport in quantum materials at diverse length and time scales [2–20]. However, despite this interest, the fundamental question of how an orderly hydrodynamic behavior on macroscales stems from a chaotic dynamics due to interactions and collisions on microscales, in particular the role of the quantum effects, has received relatively little attention. The situation is well understood for classical gases, where all moments of momentum distribution not protected by conservation laws are extremely fragile, being quickly erased after just a few (~ 1) collisions [see, e.g., [21]]. To the contrary, as discussed below, quantum gases and liquids can feature surprising collective memory effects occurring over the span of $N \gg 1$ collisions with N rapidly diverging at low temperatures. The long-time dynamics in such systems cannot be captured by a conventional hydrodynamic description that relies on a closed system of equations for the classically-conserved quantities such as local flow velocity, particle density and temperature. Instead, a full description must account for memory effects due to nonclassical quantities that are not protected by microscopic conservation laws but nevertheless can feature abnormally long lifetimes.

An early indication that such nonclassical long-lived quantities may exist in electron systems was provided by another important paper by Gurzhi [22] (see also [23]). This work emphasized the role of collinear scattering due to head-on collisions in 2D electron systems. Curiously, it was thought at the time that collinear scattering shortens quasiparticle lifetimes through speeding up the excitations' decay by a non-Fermi-liquid log factor [24–30]. Subsequent work cleared this misconception and linked the collinear scattering in 2D systems to long-lived excitations, opening way to explore a variety of collective memory effects [31–33]. These results came at a crucial juncture as 2D systems have become the focal point of ongoing efforts to achieve electron hydrodynamics [34–38]. From theoretical standpoint, the properties of 2D systems were found to lie somewhere between those of 3D and 1D systems, being sharply distinct from both. For 3D systems, the Fermi-liquid theory confirms Boltzmann's short-time memory picture with the onset of hy-

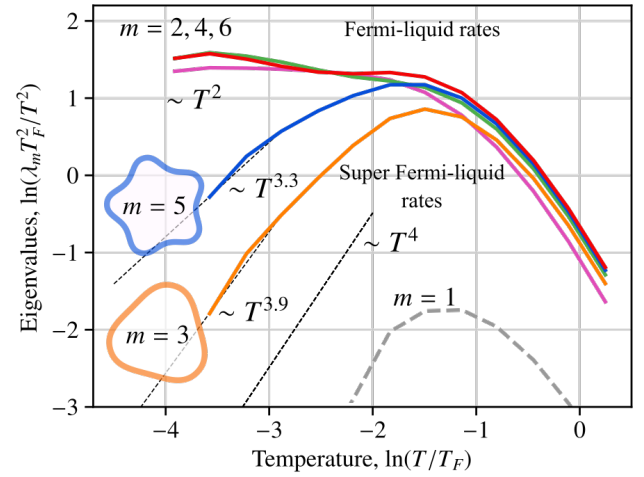


FIG. 1. Decay rates for different angular harmonics of electron velocity distribution, scaled by T^2 , vs. temperature (from [41]). Shown are dimensionless eigenvalues λ_m related to the decay rates through $\gamma_m = A p_F^2 \lambda_m$, see Eq.(32) in [41]. Double-log scale is used to facilitate comparison of disparate time scales. Decay rates for even- m harmonics obey a T^2 scaling at $T \ll T_F$. Decay rates for odd- m harmonics are suppressed below the even- m rates, showing “super-Fermi-liquid” scaling strongly deviating from T^2 . Odd- m decay rates can be approximated as T^α with $\alpha > 2$. A small nonzero rate found for velocity mode $m = 1$ is a parasitic effect (see text). An even/odd asymmetry in the rates and the suppression of decays for odd- m harmonics is clearly seen below $T \approx 0.2T_F$.

drodynamics occurring after ~ 1 quasiparticle collisions [39]. The 1D systems feature manifestly non-Boltzmann behavior, described by the Luttinger-liquid theory that predicts integrable non-ergodic behavior that extends to arbitrarily large times and distances [40]. The unique behavior in 2D Fermi systems, which is due to the dominant role of head-on collisions [22, 23, 31], deviates strongly from that in both 3D and 1D systems.

The nonclassical long-lived excitations are odd- m harmonics of the velocity distribution of fermions perturbed away from equilibrium. Recent microscopic analysis of quasiparticle scattering at a circular Fermi surface (FS) predicts quenching of the Landau T^2 damping for such

modes [41]. As illustrated in Fig.1, the quenching sets in fairly abruptly as temperature is lowered. Low-lying excitations in this system can be viewed as FS modulations evolving in space and time as

$$\delta f(\mathbf{p}, \mathbf{x}, t) \sim \sum_{m \text{ odd}} \alpha_m \cos m\theta + \beta_m \sin m\theta, \quad (1)$$

where θ is the angle parameterizing the FS and, for conciseness, we suppressed the dependence of the coefficients α_m and β_m on position, time and particle energy. The microscopic decay rates pictured in Fig.1 govern dynamics of spatially-uniform excitations, $\alpha_m, \beta_m \sim e^{-\gamma_m t}$. At low temperatures $T \ll T_F$ the lifetimes of odd- m modes greatly exceed those for the even- m ones and show strong departure from the conventional T^2 scaling.

The decay rates in Ref.[41] were obtained by a direct calculation that treats quasiparticle scattering exactly, using a method that does not rely on the small parameter $T/T_F \ll 1$. The good accuracy of the method used in [41] can be benchmarked by a residual γ_m value for the velocity mode, $m = 1$, that must vanish due to momentum conservation in two-body collisions. Here it takes a small nonzero value due to the effects of sampling the p space and inaccuracies in calculating overlaps between different states. The odd- m decay rates found for $m > 1$ display scaling $\gamma_m \sim T^\alpha$ with super-Fermi-liquid exponents $\alpha > 2$. The exponent α values were found to be close to 4, indicating a strong suppression of the odd- m rates compared to the even- m rates, $\gamma_{\text{odd}}/\gamma_{\text{even}} \sim (T/T_F)^2$. This defines a new hierarchy of lifetimes for collective modes, leading to hydrodynamics with non-Newtonian (scale-dependent) viscosity.

I. ODD-PARITY FERMI SURFACE MODULATIONS

To illustrate these properties we first focus on the two odd- m harmonics with longest lifetimes, $m = \pm 1$ and ± 3 , leaving out for the time being the harmonics with higher m . These two harmonics are singled out by a peculiar dependence of the lifetimes of excitations with different angular momenta m on temperature and m parity and magnitude that renders some excitations more long-lived than others. One characteristic property which makes odd- m excitations long-lived [33] is the even/odd difference in temperature scaling (T^2 for even m and T^4 for odd m). Another key property is that the odd- m excitations with not too large m display a steep m^4 dependence on m . This T and m dependence can be summarized as:

$$\gamma_{m \text{ odd}} \sim g \frac{T^4}{T_F^4} m^4 \ln m, \quad \gamma_{m \text{ even}} \sim g \frac{T^2}{T_F^2} \ln m, \quad (2)$$

where g is a dimensional factor that depends on the band structure [41]. The two branches of excitations, even- m and odd- m , are clearly set apart at not too large m but, as m grows, eventually merge into a parity-blind mode

at a high $m \gtrsim m_* \approx \sqrt{T_F/T}$. This behavior can be seen clearly in Fig. 1. Naturally, the dependence in Eq.(2) only applies to the part of momentum distribution that decays due to electron-electron (ee) collisions. This encompasses all harmonics with the exception of those with $m = 0, \pm 1$ that remain unchanged under ee collisions owing to the conservation of particle number and momentum.

As a result, the velocity mode $m = \pm 1$ and the third-harmonic mode $m = \pm 3$ emerge as the longest-lived excitations. The former is damped only by momentum-relaxing scattering by disorder or phonons but not by ee collisions, the latter is damped by ee collisions more weakly than any higher- m excitation (see Fig.1). In this two-mode approximation, the shear modes relevant for hydrodynamics take the form

$$\delta f(\mathbf{p}, \mathbf{x}, t) \sim \beta_1(\mathbf{x}, t) \sin \theta + \beta_3(\mathbf{x}, t) \sin 3\theta, \quad (3)$$

with θ measured from \mathbf{k} direction, with a harmonic dependence $\beta_m(\mathbf{x}, t) \sim e^{i\mathbf{k}\mathbf{x} - i\omega t}$. Here \mathbf{k} is the wavenumber describing the mode spatial dependence. After integrating out the fast-relaxing modes with $m \neq 1, 3$, we will arrive at two different hydrodynamic regimes that arise due to the appearance of a new timescale set by γ_3 :

- (i) the short-time regime $\omega, \nu k^2 \gg \gamma_3$, and
- (ii) the long-time regime $\omega, \nu k^2 \ll \gamma_3$,

where ν is the kinematic viscosity, $\nu = v_F^2/4\gamma_2$. At relatively short times $t \ll 1/\gamma_3$, i.e., in the first regime, the modes in Eq. (3) coupled by finite- k effects discussed below yield two separate viscous modes. These modes are found by diagonalizing a 2×2 mode coupling problem. As we will see, viscosity for these modes takes universal values

$$\nu_1 = \nu \frac{3 + \sqrt{5}}{2}, \quad \nu_2 = \nu \frac{3 - \sqrt{5}}{2} \quad (4)$$

satisfying $\nu_1 > \nu > \nu_2$ and having a large ratio $\nu_1/\nu_2 = (3 + \sqrt{5})/(3 - \sqrt{5}) \approx 6.9$.

The qualitative picture underpinning this regime is that quasiparticles collide at a normal Landau T^2 rate that can be estimated as γ_2 , which leads to their diffusion in space with the diffusivity ν . This diffusion, however, rather than being memory-erasing is of a memory-preserving character. Indeed, while the even- m part of velocity distribution relaxes at relatively short times $\sim \gamma_2^{-1}$, the odd- m part remains unrelaxed, producing memory effects manifested in a new hydrodynamic mode.

In the second regime the conventional viscous (Newtonian) hydrodynamics is restored. This happens at distances such that νk^2 is smaller than γ_3 :

$$L > \frac{v_F}{\sqrt{2}\gamma_2\gamma_3}. \quad (5)$$

These lengthscales are reached by a particle after undergoing many collisions, with the typical collision numbers

estimated as

$$N = \sqrt{\frac{\gamma_2}{2\gamma_3}} \sim \frac{T_F}{T} \gg 1. \quad (6)$$

The number of subsequent collisions required for the memory of a microstate to be erased diverges in the low- T limit, indicating a sharply non-Boltzmann behavior manifested as non-newtonian hydrodynamics with scale-dependent viscosity.

Turning to the analysis, we consider the most general framework describing electrons' velocity distribution by a kinetic equation linearized about equilibrium,

$$(\partial_t + \mathbf{v} \cdot \nabla) \delta f - I[\delta f] = -e\mathbf{E}(r) \cdot \frac{\partial f_0}{\partial \mathbf{p}}. \quad (7)$$

Here I is a linearized collision integral, \mathbf{E} is the electric field, and $\delta f(p, r, t) = f - f_0$ describes a state weakly perturbed away from the Fermi-Dirac equilibrium state $f_0(p) = 1/(e^{\beta(\epsilon(p) - \mu)} + 1)$. Since the perturbed distribution $\delta f(p, r, t)$ is concentrated near the Fermi surface, we can expand it in the angular harmonics as

$$\delta f(\mathbf{p}, \mathbf{r}, t) = -\frac{\partial f_0}{\partial p} \sum_m e^{im\theta} \delta f_m(p). \quad (8)$$

where θ is the angle on the Fermi surface and the dependence on \mathbf{p} in $\delta f_m(p)$ is on the modulus of \mathbf{p} .

Carrying out spatial and temporal Fourier transform gives

$$\delta f(\mathbf{p}, \mathbf{r}, t) = \sum_{\mathbf{k}, \omega} \delta f_{\omega, \mathbf{k}}(\mathbf{p}) e^{i\mathbf{k}\mathbf{r} - i\omega t}, \quad (9)$$

where ω and \mathbf{k} are frequencies and wavenumbers. The quantity $\delta f_{\omega, \mathbf{k}}(\mathbf{p})$ is in general a function of ω and \mathbf{k} determined as discussed below. Angular decomposition of $\delta f_{\omega, \mathbf{k}}(\mathbf{p})$ is identical to that in Eq.(8):

$$\delta f_{\omega, \mathbf{k}}(\mathbf{p}) = -\frac{\partial f_0}{\partial p} \sum_m e^{im\theta} \delta f_m(p). \quad (10)$$

Here we will use this expression with the angle θ on the Fermi surface measured from the direction of \mathbf{k} . For conciseness, we will suppress the dependence of δf_m on ω and \mathbf{k} . Angular harmonics defined as in Eqs. (8) and (10) are eigenfunctions of a linearized collision integral,

$$I[e^{im\theta} \delta f_m(p)] = -\gamma_m e^{im\theta} \delta f_m(p), \quad (11)$$

where the eigenvalues γ_m represent relaxation rates of individual harmonics of momentum distribution due to ee collisions [41].

The electric field $\mathbf{E}(r)$ in Eq.(7) can in general describe several distinct effects. It can be either applied externally, as in a calculation of electrical conduction, or be internal to the system, describing the effects of a non-equilibrium space charge distribution resulting from electron movement. It is therefore useful to take a moment

to clarify the role of internal \mathbf{E} fields in our problem. The internal fields habitually take on very different roles in the longitudinal and transverse response, $\mathbf{k} \parallel \mathbf{E}$ and $\mathbf{k} \perp \mathbf{E}$. In the longitudinal response, current has a finite divergence that drives density perturbations leading to charge piling up in the system bulk or edges and, at high frequency, excitation of collective plasma waves. For transverse response, to the contrary, current has zero divergence and density remains unperturbed. In this case, with density being constant and equal to that in equilibrium, hydrodynamic modes emerge that, at linear order, are unaffected by the internal fields.

While here we are interested in the transverse response that is ultimately found to be insensitive to the internal field effects, it is instructive to demonstrate the different role of internal fields in the longitudinal and transverse response by an explicit calculation. This can be done by considering Fourier harmonics of particle distribution perturbed away from equilibrium and the electric potential induced by this perturbation,

$$\mathbf{E}(\mathbf{k}) = -i\mathbf{k}U(\mathbf{k}) \sum_p \delta f(p), \quad U(\mathbf{k}) = \frac{2\pi e^2}{\kappa|\mathbf{k}|}, \quad (12)$$

where κ is the dielectric constant and \mathbf{k} is the spatial wavevector. Plugging $\mathbf{E}(\mathbf{k})$ in Eq.(7) and expanding particle distribution in angular harmonics, Eq.(9), yields a system of coupled equations for different harmonics δf_m . This problem describes both the longitudinal and transverse response, where $\delta f_m = \delta f_{-m}$ and $\delta f_m = -\delta f_{-m}$, respectively.

Here we focus on the transverse case $\mathbf{k} \perp \mathbf{E}$ (and, therefore, $\delta f_m = -\delta f_{-m}$) and show that the hybridization of the $m = \pm 1$ and $m = \pm 3$ harmonics results in modes with a scale-dependent (non-newtonian) viscosity. Since the condition for transverse modes, $\delta f_m = -\delta f_{-m}$, implies $\delta f_0 = 0$, the transverse modes are not accompanied by charge buildup. Accordingly, in this case the $m = 0$ harmonic and the internal electric field drop out. These quantities, however, would be present for the longitudinal modes such as plasmons. Both kinds of modes, transverse and longitudinal, are readily captured by writing the kinetic equation in a general form that incorporates an \mathbf{E} -field term:

$$\begin{aligned} &(\gamma_m - i\omega) \delta f_m + \frac{ikv}{2} (\delta f_{m-1} + \delta f_{m+1}) \\ &= -\frac{ievk}{2m} \frac{\partial f_0}{\partial \varepsilon} U(k) \delta f_0 (\delta_{m,1} + \delta_{m,-1}), \end{aligned} \quad (13)$$

where mode decay rates γ_m obey relations $\gamma_0, \gamma_1 = 0$ due to particle number conservation and momentum conservation. For the moment, we carry on with the general problem, Eq.(13), eventually specializing to the transverse case and discarding the $U(k)$ term.

II. NON-NEWTONIAN VISCOSITY IN A TWO-MODE MODEL

Here we derive hydrodynamic modes and viscosities for the two-mode model introduced above. We assume a small decay rate for long-lived $m = 3$ excitations,

$$\gamma_3 = \gamma' \ll \gamma^* = \min(\gamma_5, \gamma_7, \dots, \gamma_{m_{\text{even}}}). \quad (14)$$

In addition, we introduce a small momentum relaxation rate $\gamma_1 = \gamma_p$ accounting for disorder and phonon scattering, assuming a small value $\gamma_p \ll \gamma^*$.

At sufficiently long times such that $\omega \ll \gamma^*$, the even- m harmonics are mostly relaxed, giving an expression that links the even harmonics and the odd harmonics:

$$\delta f_{2m} = -\frac{ikv}{2\gamma_{2m}} (\delta f_{2m+1} + \delta f_{2m-1}). \quad (15)$$

For the odd- m harmonics, we first consider the long-lived $m = \pm 1$ and $m = \pm 3$ harmonics, which obey

$$(\gamma_p - i\omega) \delta f_{\pm 1} + \frac{ikv}{2} (\delta f_0 + \delta f_{\pm 2}) \quad (16)$$

$$= -\frac{ievk}{2m} U(k) \frac{\partial f_0}{\partial \varepsilon} \delta f_0$$

$$(\gamma' - i\omega) \delta f_{\pm 3} + \frac{ikv}{2} (\delta f_{\pm 2} + \delta f_{\pm 4}) = 0 \quad (17)$$

The above equations are true for both the transverse and longitudinal modes.

From now on we specialize to transverse modes. In this case, as noted above, density remains unperturbed, $\delta f_0 = 0$, and therefore the electric field \mathbf{E} induced by density variation, Eq.(12), vanishes. Dropping δf_0 and plugging Eqs.(15) into Eq. (16), we obtain a system of coupled equations for odd- m harmonics. Retaining the harmonics $m = \pm 3, \pm 1$ and suppressing higher- m harmonics generates coupled equations for $\delta f_{\pm 3}$ and $\delta f_{\pm 1}$ variables, which are valid at sufficiently long times and large distances corresponding to frequencies

$$\omega \ll \gamma^*. \quad (18)$$

At the same time, ω can be either smaller or greater than the rates ω_p and γ_3 , both of which are small on the scale of the higher- m rates $\gamma_5, \gamma_7, \dots, \gamma$. Introducing notation for viscosity, $\nu = v^2/4\gamma$, and solving for the velocity mode $m = 1$, we obtain a collective mode dispersion relation

$$\gamma_p - i\omega + \nu k^2 - \frac{(\nu k^2)^2}{\gamma' - i\omega + 2\nu k^2} = 0. \quad (19)$$

To clarify the behavior at long times, we compare Eq.(19) in the limit of $\gamma_p = 0$ to the Stokes equation:

$$-i\omega \delta f_1 = \Xi_{k,\omega} k^2 \delta f_1. \quad (20)$$

This yields Stokes equation with a scale-dependent (non-newtonian) viscosity

$$\Xi_{k,\omega} = \nu \frac{\nu k^2 + \gamma' - i\omega}{2\nu k^2 + \gamma' - i\omega}. \quad (21)$$

For the regime of longest times and distances — $|\omega|, \nu k^2 \ll \gamma'$ — this yields a viscous mode $i\omega = \tilde{\nu} k^2$ with a weak viscosity k dependence

$$\nu(k) = \nu \left(1 - \frac{\nu k^2}{\gamma'} + O(k^4) \right), \quad (22)$$

and one slowly-decaying mode with $i\omega \sim \gamma'$.

In the regime $\gamma' \ll |\omega|, \nu k^2 \ll \gamma$, Eq.(19) predicts two distinct viscous modes with different viscosities given in Eq.(4). As a sanity check, in the limit when the long-lived mode becomes short-lived, $\gamma' \approx \gamma$, only one (the ordinary newtonian) viscous mode survives.

Since the number of viscous modes changes with frequency and length scale, it is instructive to consider the k dependence without making any simplifying approximations. Eq.(19) yields a quadratic equation for $i\omega$ that can be solved to obtain two distinct dispersing modes:

$$i\omega = \frac{1}{2} (\gamma_p + \gamma' + 3\nu k^2) \pm \sqrt{(\nu k^2)^2 + \frac{1}{4} (\gamma' - \gamma_p + \nu k^2)^2}. \quad (23)$$

This result encompasses all asymptotic regimes discussed above. Indeed, in the long-wavelength limit $\nu k^2 \ll \gamma'$, one of the modes is damped, with $i\omega$ proportional to γ' (assuming $\gamma_p \ll \gamma'$). The second mode remains viscous in this limit and has a weakly dispersing viscosity described by Eq.(22). At larger k a pair of viscous modes with viscosities $\nu_{1,2}$ given in Eq.(4) is recovered.

This analysis demonstrates that the long-lived excitation δf_3 , coupled by k -linear terms to the velocity mode δf_1 , generates an additional nonclassical hydrodynamic mode. This points to the existence of a peculiar new regime positioned between the ordinary hydrodynamic and ballistic transport regimes, in which new hydrodynamic modes can emerge. These modes are expected to contribute to transport on equal footing with the conventional Navier-Stokes hydrodynamic modes.

Lastly, a note on the validity of the analysis involving one long-lived mode. As discussed above, accounting for δf_3 mode and ignoring δf_5 and higher-order harmonics is legitimate in the interval of temperatures for which

$$\omega \ll \gamma_5, \quad (24)$$

whereas the relation between ω and the rate γ_3 can be arbitrary. Since both the even- m rates $\gamma_2, \gamma_4, \dots$ and the odd- m rates $\gamma_7, \gamma_9, \dots$ are all greater than the rate γ_5 , the condition in Eq. (24) applies to these modes too.

III. HYDRODYNAMIC MODES FOR THE CASE OF MANY LONG-LIVED EXCITATIONS

The disparity in even and odd excitation modes becomes significantly more pronounced as temperature T decreases, as evident in Fig.1 and Eq.(2). This has two important consequences. One is an increase in the number of long-lived odd- m modes that have decay rates well

under those of the even- m modes with similar m . The number of such ‘active’ odd- m modes grows quickly as T decreases. Another consequence is a rapid increase in lifetimes of these modes, described by the decay rates that scale with temperature as $\gamma \sim T^4/T_F^4$. These rates are much smaller than the typical two-body collision rates $\gamma_2 \sim \gamma_4 \sim \dots$ that define the timescale at which the hydrodynamic description emerges. Consequently, with a decrease in T , there is a rapid expansion of the family of odd- m modes that contribute to hydrodynamics. This defines an interesting phase dominated by emerging hydrodynamic modes. To gain insight into system behavior in this new regime, here we consider hydrodynamic modes in the presence of many long-lived excitations.

As a first step, we recall why the number of ‘active’ long-lived excitations grows as T decreases and estimate the number of these excitations. This happens because, as can be seen in Fig. 1, odd harmonics with large values of m have lifetimes comparable to those of even harmonics at a high T but tend to become long-lived at a lower T . One can estimate the number of such long-lived harmonics by noticing that for any temperature T there will be a value of m that is large enough such that the corresponding odd and even harmonics are of the same order of magnitude $\gamma_{m=2p+1} \sim \gamma_{m=2p}$. This value of m sets a natural temperature-dependent limit to the number of long-lived excitations at a given temperature. In particular, the value of m for which odd and even rates in Eq. (2) become of the same order of magnitude is $m_* \approx \sqrt{T_F/T}$.

In the case when several such long-lived excitations are present, determining the change of viscosity with scale becomes more complicated. To address this question, we consider an n -mode problem, where $n > 1$ such excitations are present simultaneously. For simplicity, at first we will take their decay rates to be negligibly small. This corresponds to frequencies in the intermediate range

$$\gamma_p, \gamma_3 \dots \gamma_{2n+1} < \omega < \gamma_{2n+3} \quad (25)$$

As above, we eliminate the fast-relaxing even- m harmonics from consideration by substituting Eq.(15) into Eq.(13), which yields a closed-form system of equations of motion for odd- m excitations.

For the first n modes these equations are

$$-i\omega \delta f_{2m+1} = -\nu k^2 (2\delta f_{2m+1} + \delta f_{2m-1} + \delta f_{2m+3}) \quad (26)$$

for $0 < m \leq n$. From the form of these equations it is evident that n hydrodynamic modes are present in this case, since all the solutions that satisfy Eq.(26) have the relaxation rates proportional to νk^2 . Determining the spectrum of viscosities in the system therefore is equivalent

to diagonalizing an $n \times n$ matrix

$$\begin{bmatrix} 1 & 1 & 0 & \dots \\ 1 & 2 & 1 & \\ 0 & 1 & 2 & \\ \vdots & & \ddots & \vdots \\ & & & 2 & 1 & 0 \\ & & & 1 & 2 & 1 \\ & & \dots & 0 & 1 & 2 \end{bmatrix}. \quad (27)$$

The eigenstates and eigenvalues for this matrix are readily found by a comparison to a 1D tight binding problem on an infinite line

$$H = \sum_x 2|x\rangle\langle x| + |x\rangle\langle x+1| + |x+1\rangle\langle x| \quad (28)$$

where x is an integer. This problem has plane-wave eigenstates $\psi(x) = e^{ipx}$ with the eigenvalues

$$\lambda_k = 2 + 2\cos p$$

degenerate in p and $-p$

To derive the problem stated in Eq.(27), we analyze state vectors $\psi(x)$ that fulfill two auxiliary anti-symmetry conditions specifically chosen to replicate the matrix’s structure described in Eq.(27) with “1” in the upper-left corner and “2” in the lower-right corner. The two anti-symmetry conditions are imposed relative to the points $x = 1/2$ and $x = n + 1$. Indeed, focusing on the solutions anti-symmetric relative to $x = 1/2$,

$$\psi(1) = -\psi(0), \psi(2) = -\psi(-1), \dots$$

yields equations

$$\lambda\psi(1) = \psi(1) + \psi(2), \quad \lambda\psi(2) = 2\psi(2) + \psi(1) + \psi(3), \dots$$

identical to those described by the upper left part of our matrix. At the same time, the anti-symmetry condition relative to $x = n + 1$,

$$\psi(n+1) = 0, \psi(n) = -\psi(n+2), \psi(n-1) = -\psi(n+3), \dots$$

yields equations

$$\begin{aligned} \lambda\psi(n) &= 2\psi(n) + \psi(n-1), \\ \lambda\psi(n-1) &= 2\psi(n-2) + \psi(n-1) + \psi(n-3), \dots \end{aligned}$$

identical to those described by the lower right part of the matrix.

Combining the two anti-symmetry conditions selects n plane-wave solutions of the form $\psi(x) \sim \sin p_j(x - 1/2)$ with discrete p_j values

$$p_j = \frac{2\pi j}{2n+1}, \quad j = 1 \dots n. \quad (29)$$

The eigenvalues for these modes are $2 + 2\cos p_j$, yielding n viscous modes with viscosity values

$$\nu_j = 2\nu \left[1 + \cos \left(\frac{2\pi j}{2n+1} \right) \right], \quad j = 1, \dots, n. \quad (30)$$

This result is valid for any $n \geq 2$. As a consistency check, for $n = 2$ the result found above, $\nu_{1,2} = \nu(3 \pm \sqrt{5})/2$, is recovered.

These expressions for ν_j imply that the largest viscosity ν_j converges to a n -independent value 4ν as n grows. In contrast, the smallest viscosity ν_j scales inversely with n^2 : $\min \nu_j \sim \nu/n^2$. Therefore, while a total of n modes will be present, only a subset of those that have large enough viscosities will feature a predominantly hydrodynamic behavior. The low-viscosity modes will be masked by small but non-zero decay rates $\gamma_3, \gamma_5, \dots, \gamma_{2n+2}$.

We also note that a more realistic model can be constructed by letting different odd- m harmonics to have different nonzero decay rates γ_m , and their number n to scale with temperature. This generalized n -mode problem can be used to understand the interplay between relaxation rates for different harmonics and the number of ‘active’ viscous modes controlling carrier transport. This interplay governs several key aspects of transport, in particular the conductance temperature dependence.

IV. NONLOCAL CONDUCTIVITY DUE TO HYDRODYNAMICS MODES

Given the multitude of new hydrodynamic modes originating from long-lived excitations, it is interesting to explore how these modes impact transport in a realistic geometry. To set the stage for this discussion, we recall that the standard treatment by Gurzhi of a viscous electron flow in a long strip predicts a temperature dependent conductance due to a viscous mode that grows with temperature as T^2 [1]. This reflects the T dependence of e-e scattering that enters the Navier-Stokes electron viscosity. The T^2 scaling arises when the viscosity is found without accounting for the collinear scattering effects. Collinear scattering creates long-lived excitations and results in multiple hydrodynamic modes. As demonstrated below, these modes give a unique contribution to the conductance that mimics some aspects of the conductance predicted in Gurzhi’s theory but, in general, has a different dependence on system parameters such as temperature and strip width. A non-Gurzhi T dependence, if observed, can provide a signature of the new hydrodynamic modes.

As we saw above, the long-lived excitations are manifested in additional hydrodynamic modes in an infinite system. Now we consider how these modes impact transport in a realistic geometry. Namely, we consider an infinite strip of width w with diffuse carrier scattering at the boundaries and show that the extra hydrodynamic modes lead to a unique dependence of the DC conductivity on system parameters. To compute the electrical conductivity governed by Eq. (13) with the new boundary conditions we first consider an auxiliary problem of conduction in an infinite plane, where \mathbf{k} is taken to be perpendicular to \mathbf{E} .

This auxiliary problem is motivated by the following

considerations: the steady-state DC current flowing in a long strip geometry must be constant along the strip and vary in the direction perpendicular to the strip. Therefore, in this geometry all current-carrying modes have \mathbf{k} perpendicular to the strip and \mathbf{E} along the strip. To describe conduction in this system, we add an extra term to Eq.(13) that describes a fictitious internal electric field localized at the strip boundary which couples to δf_m modes. This field has components E_{\parallel} along \mathbf{k} and E_{\perp} perpendicular to \mathbf{k} , entering transport equations as an extra term in the RHS of Eq.(13) of the form

$$-\frac{ev_F}{2} \frac{\partial f_0}{\partial \varepsilon} [E_{\parallel} (\delta_{m,1} + \delta_{m,-1}) + iE_{\perp} (\delta_{n,-1} - \delta_{n,+1})],$$

where E_{\parallel} is a component of external electric field along \mathbf{k} and E_{\perp} is a component perpendicular to \mathbf{k} . As it was mentioned above, in our case \mathbf{E} is perpendicular to \mathbf{k} , so we can set $E_{\parallel} = 0$, and $E_{\perp} = E_0$.

Combined with the transverse mode condition $\delta f_m = -\delta f_{-m}$, equations for δf_m , Eq.(13), can be solved recursively [see Appendix and Ref.[20]], yielding a continued fraction expression for conductivity

$$\sigma_{\perp}(k) = \frac{n_0 e^2}{m} \frac{1}{\gamma_p + \frac{z}{\gamma_2 + \frac{z}{\gamma_3 + \frac{z}{\gamma_4 + \dots}}}}, \quad z = v_F^2 k^2 / 4, \quad (31)$$

where we expressed carrier density $n_0 = \frac{p_F^2}{4\pi\hbar^2}$ through Fermi momentum and set $\omega = 0$ for the DC response. Starting with this general result, which is true for any decay rate values γ_m , allows to embed our analysis in a wider context. The k -dependent conductivity describes a nonlocal conduction response with the nonlocality accounting for carrier movement accompanied by velocity distribution relaxation with the rates γ_m that are different for different angular harmonics.

The result in Eq.(31) can be readily applied to the n -mode problem with n long-lived excitations introduced above, for which the viscous mode spectrum, Eq.(30), was derived. In this model the odd- m rates $\gamma_3, \gamma_5, \dots, \gamma_{2n+1}$ were taken to be zero, whereas for all other modes the rates equal γ except for the $m = 1$ rate that takes a small nonzero value $\gamma_1 = \gamma_p \ll \gamma$. For $i > 2n + 1$, the tail of the infinite continued fraction in Eq.(31) can be evaluated exactly with the help of the identity

$$\frac{z}{\gamma + \frac{z}{\gamma + \dots}} = \frac{\gamma}{2} \left(\sqrt{1 + \frac{4z}{\gamma^2}} - 1 \right) \quad (32)$$

Plugging this result in Eq.(31) gives

$$\sigma_{\perp}(k) = \frac{n_0 e^2}{m} \frac{1}{\gamma_p + \frac{z}{(n+1)\gamma + \frac{\gamma}{2} \left(\sqrt{1 + \frac{4z}{\gamma^2}} - 1 \right)}} \quad (33)$$

$$\approx \frac{n_0 e^2}{m} \frac{1}{\gamma_p + \frac{z}{(n+1)\gamma}} \quad (34)$$

In the last line we suppressed the quantity in Eq.(32), which is small in the regime of interest, $v_F k \ll \gamma$, away

from the ballistic transport. We are particularly interested in exploring the lengthscales $\gamma', \gamma_p \ll \nu k^2 \ll \gamma$ in between the conventional hydrodynamic and ballistic regimes where the effects of additional viscous modes take on a central role. Accordingly, setting $\gamma_p = 0$ yields a simple expression for k -dependent conductivity

$$\sigma_{\perp}(k) = \frac{e^2 n_0}{m} \frac{n+1}{\nu k^2}. \quad (35)$$

This result coincides in form with the conductivity derived from Navier-Stokes equation multiplied by a factor $n+1$, reflecting an enhancement in conductivity due to the presence of the additional hydrodynamic modes. Interestingly, while the viscous modes found above feature a wide distribution of viscosity values, Eq.(30), their net contribution to conduction carries little information about this complexity. Instead, it matches the conduction of a single conventional hydrodynamic mode, recovered from Eq.(30) at $n=0$, multiplied by the number of the long-lived modes $n+1$.

V. TRANSPORT IN A STRIP GEOMETRY

Next, we use the expression for $\sigma_{\perp}(k)$ found in an infinite plane, Eq.35, to determine current distribution and conductivity in a long strip,

$$0 < x < w, \quad -\infty < y < \infty,$$

where the coordinate axis x is directed perpendicular to the strip, whereas the electric field and current are directed along the strip. To tackle the boundary conditions we employ the method outlined in Ref.[32], wherein an electric field is introduced at the strip boundaries of the form chosen to achieve zero current at the boundary. Physically, the auxiliary electric field term at boundary describes current dissipation due to carrier momentum relaxation at the boundary. Writing this auxiliary field as $\delta E = -\alpha j$, with j a yet unknown current at the boundary and the minus sign describing momentum relaxation at the boundary, yields a self-consistent current-field relation

$$E'(x) = E_0 - \alpha \sum_n j(x_n) \delta(x - x_n). \quad (36)$$

Here $x_n = wn$ describes strip boundaries periodically replicated throughout $-\infty < x < \infty$. The electric field and current, directed along the strip, vary across the strip but are constant along the strip. The relation between current and field is therefore provided by the quantity $\sigma_{\perp}(k)$ discussed above.

The idea of the method is to assume a current-dependent E' that differs from an externally applied E by a boundary term as given above, and solve Eq.(36) together with the nonlocal current-field relation

$$j(x) = \int_{-\infty}^{\infty} dx' \sigma(x-x') E'(x') \quad (37)$$

where we introduced nonlocal conductivity $\sigma(x-x') = \int_{-\infty}^{\infty} \frac{dk}{2\pi} e^{ik(x-x')} \sigma_{\perp}(k)$. The mathematical procedure involves solving for the current response governed by a nonlocal conductivity exactly for $j(x)$ as a function of α and E_0 , followed by taking the limit of $\alpha \rightarrow \infty$ to ensure that the current vanishes at the boundaries $x = x_n$. This yields a one-dimensional integral equation, Eq.(37), for the current distribution on a line $-\infty < x < \infty$. The solution of this integral equation describes current distribution that is governed by $\sigma_{\perp}(k)$ within the strip and, in the limit $\alpha \rightarrow \infty$, vanishes at the boundary. The integral equation, Eq.(37), is readily solved for an arbitrary $\sigma_{\perp}(k)$ dependence by Fourier transform [see Ref.[32]]. Since our expression for $\sigma_{\perp}(k)$ in Eq. (35) has the same $1/k^2$ form as the viscous conductivity in the Stokes' hydrodynamic limit, the results of Ref.[32] can be applied directly. This yields a current distribution $j(x)$ in the strip that has a parabolic profile familiar for the viscous Poiseuille flow. However, because of a simultaneous presence of n hydrodynamic modes the current-field relation is distinct from Gurzhi's hydrodynamic limit conductivity:

$$j(x) = \sigma_{\text{eff}} E_0 \frac{x}{w} \left(1 - \frac{x}{w}\right), \quad \sigma_{\text{eff}} = \frac{\gamma e^2 m w^2}{12\pi \hbar^2} (n+1). \quad (38)$$

This result coincides with the Gurzhi's hydrodynamic conductivity multiplied by a factor $n+1$, whereas in the absence of the odd- m long-lived modes, $n=0$, it matches exactly the result of Gurzhi's theory.

Below we use these results to describe different regimes arising in our problem. Since in the strip geometry the characteristic wavenumber is $k \sim 1/w$, we obtain the applicability condition of the result in Eq.(38) by recalling that $\gamma' \ll \nu k^2 \ll \gamma$. This gives

$$\sqrt{\gamma' \gamma} \ll \frac{v_F}{w} \ll \gamma. \quad (39)$$

This inequality implies the existence of three different transport regimes occurring for different strip width values:

1. The ballistic regime, which occurs for relatively small strip widths w such that

$$\gamma \ll \frac{v_F}{w}. \quad (40)$$

In this case the conductivity is in the ballistic regime and the conductivity of the strip is large.

2. The multi-mode hydrodynamic regime: w is such that

$$\sqrt{\gamma' \gamma} \ll \frac{v_F}{w} \ll \gamma. \quad (41)$$

In this case the conductivity will be enhanced by a factor of $(n+1)$ in comparison to the conventional hydrodynamic regime:

$$\sigma_{\text{eff}} = \frac{\gamma e^2 n_0 w^2}{3m v_F^2} (n+1). \quad (42)$$

3. The conventional hydrodynamic regime occurs when the value of w is very large, such that

$$\frac{v_F}{w} \ll \sqrt{\gamma'\gamma}. \quad (43)$$

The conductivity in this regime corresponds to the standard Gurzhi's result:

$$\sigma_{\text{eff}} = \frac{\gamma e^2 n_0 w^2}{3m v_F^2}. \quad (44)$$

We therefore see that as w grows the system does not transition directly from a ballistic into a hydrodynamic regime, but features a new regime with an enhanced conductivity. Combining it with the fact that both number of long-lived modes and the decay rates γ and γ' depend on temperature, this opens a possibility of a novel temperature scaling of σ_{eff} occurring in the regime with several active hydrodynamic modes.

In this particular model, however, the temperature scaling remains trivial: the new regime has the same scaling $\sigma_{\text{eff}} \sim T^2$, as the conventional hydrodynamic regime. The difference in conductivity only comes from the constant factor increase relative to the hydrodynamic regime. Since $\gamma_{2m} = \gamma \sim T^2$ in this model, the Eq. (44) yields $\sigma_{\text{eff}} \sim T^2$. Therefore, one would only find non-trivial temperature scaling at the values of parameters that correspond to the transition between the regimes. The less trivial information obtained from this model are the temperature-dependent boundaries between the regimes. Let's assume that both γ and γ' are given by

$$\gamma = g \frac{T^2}{T_F^2}, \quad \gamma' = g \frac{T^4}{T_F^4}. \quad (45)$$

Then the regime with several hydrodynamic modes takes place when

$$g \frac{T^3}{T_F^3} \ll \frac{v_F}{w} \ll g \frac{T^2}{T_F^2}. \quad (46)$$

Therefore, ballistic regime will be dominant at $T \ll T_F \sqrt{v_F/gw}$, the transient regime with multiple hydrodynamic modes will correspond to $T_F \sqrt{v_F/gw} \ll T \ll$

$T_F \sqrt[3]{v_F/gw}$, which can span a wide range of temperatures if $v_F/gw \ll 1$. Finally, at large temperatures $T_F \sqrt[3]{v_F/gw} \ll T$ the conventional hydrodynamic regime dominates the transport.

We note that the model with a fixed value of n is only applicable in a relatively narrow range of temperatures in application to realistic systems. Therefore for different temperatures the value of n will change in a system that is described by decay rates as in Fig. 1. Effective dependence of n on T will lead to the different temperature scaling in the regime with a large n . In the contrary to the constant n model and in support of things said above, our preliminary results show that if γ_{2m+1} depends on m , the temperature scaling in the newly discovered regime will diverges from the conventional hydrodynamic T^2 scaling in Gurzhi's theory represents an interesting topic for future work.

In summary, restricted phase space for quasiparticle scattering near the Fermi level renders quasiparticle scattering in 2D Fermi gases a highly collinear process even when the microscopic interactions have a weak angular dependence. The unusual kinetics originating in this regime is relevant for a variety of 2D systems, in particular those where small carrier density and small kinetic energy make electron-electron collisions a dominant scattering mechanism that overwhelms other carrier relaxation pathways. The resulting carrier dynamic features long-lived excitations that manifest themselves through new hydrodynamic modes with non-newtonian (scale-dependent) viscosity. This leads to a coexistence of multiple viscous modes impossible in conventional fluids, providing a clear testable signature of the unique behavior originating from long-lived excitations in 2D electron fluids.

This work was supported by the Science and Technology Center for Integrated Quantum Materials, NSF Grant No.DMR1231319; Army Research Office Grant W911NF-18-1-0116; US-Israel Binational Science Foundation Grant No.2018033; and Bose Foundation Research fellowship.

[1] R. N. Gurzhi, Sov. Phys. Usp. 11, 255 (1968). DOI 10.1070/PU1968v011n02ABEH003815
[2] M. Müller, J. Schmalian, L. Fritz, Graphene: a nearly perfect fluid. Phys. Rev. Lett. 103, 2-5 (2009).
[3] A. Tomadin, G. Vignale, M. Polini, A Corbino disk viscometer for 2D quantum electron liquids Phys. Rev. Lett. 113, 235901 (2014).
[4] A. Principi, G. Vignale, M. Carrega, M. Polini, Bulk and shear viscosities of the two-dimensional electron liquid in a doped graphene sheet Phys. Rev. B 93, 125410 (2016)
[5] T. Scaffidi, N. Nandi, B. Schmidt, A. P. Mackenzie, J. E.

Moore, Hydrodynamic electron flow and Hall viscosity. Phys. Rev. Lett. 118, 226601 (2017).
[6] A. Lucas, K. C. Fong, Hydrodynamics of electrons in graphene, J. Phys.: Condens. Matter 30 053001 (2018).
[7] K. A. Guerrero-Becerra, F. M. D. Pellegrino, M. Polini, Magnetic hallmarks of viscous electron flow in graphene. Phys. Rev. B 99, 041407 (2019).
[8] B. N. Narozhny, M. Schütt, Magnetohydrodynamics in graphene: Shear and Hall viscosities. Phys. Rev. B 100, 035125 (2019).
[9] P. S. Alekseev, A. P. Dmitriev, Viscosity of two-

- dimensional electrons. Phys. Rev. B 102, 241409 (2020)
- [10] R. Toshio, K. Takasan, N. Kawakami, Anomalous hydrodynamic transport in interacting noncentrosymmetric metals. Phys. Rev. Res. 2, 032021 (2020).
- [11] B. N. Narozhny, I. V. Gornyi, M. Titov, Hydrodynamic collective modes in graphene. Phys. Rev. B 103, 115402 (2021).
- [12] E. H. Hasdeo, J. Ekstrom, E. G. Idrisov, T. L. Schmidt, Electron hydrodynamics of two-dimensional anomalous Hall materials. Phys. Rev. B 103, 125106 (2021).
- [13] M. Qi, A. Lucas, Distinguishing viscous, ballistic, and diffusive current flows in anisotropic metals, Phys. Rev. B 104 (19), 195106 (2021)
- [14] C. Q. Cook, A. Lucas, Viscometry of electron fluids from symmetry, Phys. Rev. Lett. 127 (17), 176603 (2021)
- [15] D. Valentinis, J. Zaanen, D. van der Marel Propagation of shear stress in strongly interacting metallic Fermi liquids enhances transmission of terahertz radiation Sci. Rep. 11, 7105 (2021)
- [16] D. Valentinis, Optical signatures of shear collective modes in strongly interacting Fermi liquids Phys. Rev. Research 3, 023076 (2021)
- [17] J. Hofmann and S. Das Sarma, Collective modes in interacting two-dimensional tomographic Fermi liquids, Phys. Rev. B 106, 205412 (2022)
- [18] H. Guo, E. Ilseven, G. Falkovich, and L. Levitov, Higher-than-ballistic conduction of viscous electron flows, Proc. Natl. Acad. Sci. U.S.A. 114, 3068 (2017).
- [19] A. V. Shytov, J. F. Kong, G. Falkovich, and L. S. Levitov, Particle Collisions and Negative Nonlocal Response of Ballistic Electrons, Phys. Rev. Lett. 121, 176805 (2018).
- [20] K. G. Nazaryan, L. S. Levitov, Robustness of vorticity in electron fluids, arXiv:2111.09878.
- [21] R. L. Liboff, Kinetic Theory: Classical, Quantum, and Relativistic Descriptions (Springer-Verlag, New York, 2003)
- [22] R. N. Gurzhi, A. N. Kalinenko, and A. I. Kopeliovich, Electron-Electron Collisions and a New Hydrodynamic Effect in Two-Dimensional Electron Gas, Phys. Rev. Lett. 74, 3872 (1995)
- [23] H. Buhmann, L. W. Molenkamp, 1D diffusion: a novel transport regime in narrow 2DEG channels, Physica E 12, 715-718 (2002)
- [24] C. Hodges, H. Smith, and J. W. Wilkins, Effect of Fermi Surface Geometry on Electron-Electron Scattering, Phys. Rev. B 4, 302 (1971).
- [25] A. V. Chaplik, Energy Spectrum and Electron Scattering Processes in Inversion Layers, Zh. Eksp. Teor. Fiz. 60, 1845-1852 (1971) [English translation - Sov. Phys. JETP 33, 997 (1971).]
- [26] P. Bloom, Two-dimensional Fermi gas, Phys. Rev. B 12, 125 (1975).
- [27] G. F. Giuliani and J. J. Quinn, Lifetime of a quasiparticle in a two-dimensional electron gas, Phys. Rev. B 26, 4421 (1982).
- [28] L. Zheng and S. Das Sarma, Coulomb scattering lifetime of a two-dimensional electron gas, Phys. Rev. B 53, 9964 (1996).
- [29] D. Menashe, B. Laikhtman, Quasiparticle lifetime in a two-dimensional electron system in the limit of low temperature and excitation energy, Phys. Rev. B 54, 11561 (1996)
- [30] A. V. Chubukov and D. L. Maslov, Phys. Rev. B 68, 155113 (2003).
- [31] P. J. Ledwith, H. Guo, L. Levitov, Angular Superdiffusion and Directional Memory in Two-Dimensional Electron Fluids, arXiv:1708.01915
- [32] P. Ledwith, H. Guo, A. Shytov, L. Levitov Tomographic Dynamics and Scale-Dependent Viscosity in 2D Electron Systems, Phys. Rev. Lett. 123, 116601 (2019).
- [33] P. J. Ledwith, H. Guo, L. Levitov, The Hierarchy of Excitation Lifetimes in Two-Dimensional Fermi Gases, Ann. Phys. 411, 167913 (2019).
- [34] J. A. Sulpizio, L. Ella, A. Rozen, J. Birkbeck, D. J. Perello, D. Dutta, M. Ben-Shalom, T. Taniguchi, K. Watanabe, T. Holder, R. Queiroz, A. Principi, A. Stern, T. Scaffidi, A. K. Geim, S. Ilani, Visualizing Poiseuille flow of hydrodynamic electrons Nature 576, 75-79 (2019).
- [35] M. J. H. Ku, T. X. Zhou, Q. Li, Y. J. Shin, J. K. Shi, C. Burch, L. E. Anderson, A. T. Pierce, Y. Xie, A. Hamo, U. Vool, H. Zhang, F. Casola, T. Taniguchi, K. Watanabe, M. M. Fogler, P. Kim, A. Yacoby, R. L. Walsworth, Imaging viscous flow of the Dirac fluid in graphene Nature 583, 537-541 (2020).
- [36] B. A. Braem, F. M. D. Pellegrino, A. Principi, M. Roosli, C. Gold, S. Hennel, J. V. Koski, M. Berl, W. Dietsche, W. Wegscheider, M. Polini, T. Ihn, and K. Ensslin, Scanning gate microscopy in a viscous electron fluid Phys. Rev. B 98, 241304(R) (2018).
- [37] U. Vool, A. Hamo, G. Varnavides, Y. Wang, T. X. Zhou, N. Kumar, Y. Dovzhenko, Z. Qiu, C. A. C. Garcia, A. T. Pierce, J. Gooth, P. Anikeeva, C. Felser, P. Narang, A. Yacoby, Imaging phonon-mediated hydrodynamic flow in WTe₂ Nature Physics 17, 1216-1220 (2021).
- [38] Direct observation of vortices in an electron fluid A. Aharon-Steinberg, T. Volkl, A. Kaplan, A. K. Pariari, I. Roy, T. Holder, Y. Wolf, A. Y. Meltzer, Y. Myasoev, M. E. Huber, B. Yan, G. Falkovich, L. S. Levitov, M. Hucker, E. Zeldov Nature 607, 74-80 (2022).
- [39] G. Baym, C. Pethick, Landau Fermi-Liquid Theory: Concepts and Applications (Wiley, 1991)
- [40] T. Giamarchi, Quantum Physics in One Dimension, Clarendon Press, Oxford, 2004.
- [41] S. Kryhin, L. Levitov, Collinear scattering and long-lived excitations in two-dimensional electron fluids, arXiv:2112.05076
- [42] J. Hofmann, and U. Gran, Anomalous long lifetimes in two-dimensional Fermi liquids, arXiv preprint arXiv:2210.16300 (2022)

APPENDIX: SCALE DEPENDENT CONDUCTIVITY AND CONTINUED FRACTIONS

Here we derive a general relation between nonlocal conductivity $\sigma(k)$ and the relaxation rates γ_m for the angular harmonics of carrier distribution, which is used in Eq.31 and subsequent discussion in the main text. As a starting point, we use the Boltzmann kinetic equation for electrons in the presence of an external electric field, linearized in small deviations of carrier distribution from equilibrium:

$$(\partial_t + \mathbf{v} \cdot \nabla_{\mathbf{x}} - I) \delta f_{\mathbf{p}}(t, \mathbf{x}) = -e E \nabla_{\mathbf{p}} f_{\mathbf{p}}^{(0)} \quad (\text{A1})$$

where I is the collision operator, $f_{\mathbf{p}}^{(0)}$ is the equilibrium distribution, and the electric field term can be expressed through carrier velocity as $\mathbf{E} \nabla_{\mathbf{p}} f_{\mathbf{p}}^{(0)} = \mathbf{E} \mathbf{v} \frac{\partial f_{\mathbf{p}}^{(0)}}{\partial \epsilon}$. The perturbed distribution can be decomposed into a sum of cylindrical harmonics as $\delta f_{\mathbf{p}} = e^{i\mathbf{k}\mathbf{x} - i\omega t} \sum_m \delta f_m e^{im\theta}$, where θ is the azimuthal angle on the Fermi surface. Due to the cylindrical symmetry, the harmonics $\delta f_m e^{im\theta}$ are eigenfunctions of the collision operator,

$$I \delta f_m e^{im\theta} = -\gamma_m \delta f_m e^{im\theta}, \quad (\text{A2})$$

where γ_m are relaxation rates originating from microscopic processes of carrier scattering and collisions. In particular, $\gamma_1 = \gamma_p$ describes momentum relaxation due to disorder or phonon scattering, γ_2 is due to electron-electron collisions, $\gamma_0 = 0$ due to particle number conservation, and so on. The key observation is that using the basis $\delta f_m e^{im\theta}$ the problem can be brought to the form described by a tridiagonal matrix, a representation in which a closed-form solution for conductivity $\sigma(k)$ can be given in terms of continued fractions. This representation is obtained by noting that the terms $\mathbf{v}\mathbf{k}$ and $\mathbf{v}\mathbf{E}$, when rewritten in the angular harmonics basis, have nonzero matrix elements only between harmonics m and $m \pm 1$. This is made apparent by the identities

$$\begin{aligned} \mathbf{v}\mathbf{k} &= \frac{v}{2} (k_x + ik_y) e^{-i\theta} + \frac{v}{2} (k_x - ik_y) e^{i\theta} \\ &= \zeta e^{-i\theta} + \bar{\zeta} e^{i\theta} \end{aligned} \quad (\text{A3})$$

$$\begin{aligned} e\mathbf{v}\mathbf{E} &= \frac{ev}{2} (E_x + iE_y) e^{-i\theta} + \frac{ev}{2} (E_x - iE_y) e^{i\theta} \\ &= \mathcal{E} e^{-i\theta} + \bar{\mathcal{E}} e^{i\theta} \end{aligned} \quad (\text{A4})$$

where we introduced $\zeta = v(k_x + ik_y)/2$, $\mathcal{E} = ev(E_x + iE_y)/2$. Accordingly, the Boltzmann equation turns into a system of coupled linear equations:

$$\gamma_m \delta f_m + \zeta \delta f_{m+1} + \bar{\zeta} \delta f_{m-1} = \frac{\partial f_{\mathbf{p}}^{(0)}}{\partial \epsilon} (\mathcal{E} \delta_{m,-1} + \bar{\mathcal{E}} \delta_{m,1}) \quad (\text{A5})$$

This problem describes a response of variables δf_m to the “source” $\mathcal{E} \delta_{m,-1} + \bar{\mathcal{E}} \delta_{m,1}$.

To solve these equations, we first limit the discussion to electric field perpendicular to the wave vector. We consider the source term with $m = 1$, adding the contribution of the source term with $m = -1$ later. We introduce $\alpha_m = i\delta f_{m+1}/\delta f_m$, which brings equations with $m > 1$ to the form

$$\gamma_m + \zeta \alpha_m - \frac{\bar{\zeta}}{\alpha_{m-1}} = 0 \quad (\text{A6})$$

These equations give a simple recursion equation $\alpha_{m-1} = \frac{\bar{\zeta}}{\gamma_m + \zeta \alpha_m}$, which can be solved iteratively over $m+1, m+2, \dots$ giving a continued fraction

$$\alpha_{m-1} = \frac{\bar{\zeta}}{\gamma_m + \frac{|\zeta|^2}{\gamma_{m+1} + \frac{|\zeta|^2}{\gamma_{m+2} + \dots}}} \quad (\text{A7})$$

Similarly, for $m < 1$ we define $\alpha'_m = i\delta f_{m-1}/\delta f_m$ and obtain

$$\alpha'_{m+1} = \frac{\zeta}{\gamma_m + \frac{|\zeta|^2}{\gamma_{m-1} + \frac{|\zeta|^2}{\gamma_{m-2} + \dots}}} \quad (\text{A8})$$

Now, the harmonic δf_1 can be found from the $m = 1$ equation

$$\gamma_1 \delta f_1 + i\zeta \delta f_2 + i\bar{\zeta} \delta f_0 = \frac{\partial f_{\mathbf{p}}^{(0)}}{\partial \epsilon} \mathcal{E}. \quad (\text{A9})$$

Rewriting it as $\delta f_1 (\gamma_1 + \zeta \alpha_1 + \bar{\zeta} \alpha'_1) = \frac{\partial f_{\mathbf{p}}^{(0)}}{\partial \epsilon} \mathcal{E}$ and substituting the continued fractions for α_1 and α'_1 yields

$$\begin{aligned} \delta f_1 &= \frac{\partial f_{\mathbf{p}}^{(0)}}{\partial \epsilon} \frac{\mathcal{E}}{\gamma_1 + \frac{|\zeta|^2}{\gamma_2 + \frac{|\zeta|^2}{\gamma_3 + \frac{|\zeta|^2}{\gamma_4 + \dots}}} + \frac{|\zeta|^2}{\gamma_0 + \frac{|\zeta|^2}{\gamma_{-1} + \frac{|\zeta|^2}{\gamma_{-2} + \dots}}}} \\ &= \frac{\partial f_{\mathbf{p}}^{(0)}}{\partial \epsilon} \frac{\mathcal{E}}{2\gamma_1 + \frac{2|\zeta|^2}{\gamma_2 + \frac{|\zeta|^2}{\gamma_3 + \frac{|\zeta|^2}{\gamma_4 + \dots}}}}, \end{aligned} \quad (\text{A10})$$

where we used the identities $\gamma_{-m} = \gamma_m$ and $\gamma_0 = 0$, accounting for the inversion symmetry and particle number conservation. The contribution of the $m = -1$ source term, found in a similar manner, is given by an expression identical to Eq.(A10) up to a replacement of \mathcal{E} with $\bar{\mathcal{E}}$.

Now it is straightforward to obtain the nonlocal conductivity by combining the current density $j_{y,k} = ev\nu_0 \oint (d\theta/2\pi) \sin \theta \delta f(\theta)$ and the definition of conductivity $\mathbf{j}_{\mathbf{k}} = \sigma(k, \omega) \mathbf{E}_{\mathbf{k}}$. In the static limit $\omega = 0$ we find

$$\sigma(k) = \frac{D}{\gamma_1 + \Gamma(k)}, \quad \Gamma(k) = \frac{z}{\gamma_2 + \frac{z}{\gamma_3 + \frac{z}{\gamma_4 + \dots}}}, \quad (\text{A11})$$

with $D = ne^2/m$ the Drude weight and $z = k^2 v^2/4$.

It is instructive to consider an example of equal rates $\gamma_2 = \gamma_3 = \gamma_4 = \dots = \gamma$ for which the quantity $\Gamma(k)$ can be evaluated in a closed form. Using a recursion relation $\Gamma(k) = z/(\gamma + \Gamma(k))$ we find

$$\Gamma(k) = \frac{-\gamma + \sqrt{\gamma^2 + k^2 v^2}}{2}. \quad (\text{A12})$$

This gives a scale-dependent conductivity

$$\sigma(k) = \frac{2D}{2\gamma_p + \sqrt{v^2 k^2 + \gamma^2} - \gamma}, \quad (\text{A13})$$

where we replaced γ_1 with the momentum relaxation rate γ_p to make our notations agree with those in the main text. The model describes the viscous and ballistic regimes, and the crossover between these regimes at the lengthscales corresponding to $kv \sim \gamma$.

So far we considered the transverse conductivity arising for $\mathbf{E} \perp \mathbf{k}$. A straightforward generalization of the

above derivation for an arbitrary orientation of electric field relative to the wave vector yields an additional tensor structure $\delta_{\alpha\alpha'} - \hat{k}_\alpha \hat{k}_{\alpha'}$. This tensor structure ensures

that the electric field component parallel to the wave vector \mathbf{k} is screened out and does not produce a DC current.